Physica A 527 (2019) 121309

Contents lists available at ScienceDirect

Physica A

journal homepage: www.elsevier.com/locate/physa

Stochastic dynamical systems always undergo trending mechanisms of transition to criticality

Denis M. Filatov [a,b,*], Alexey A. Lyubushin [b]

[a] Sceptica Scientific Ltd, Carpenter Court, 1 Maple Road, Bramhall, Stockport, Cheshire SK7 2DH, UK
[b] Institute of Physics of the Earth, Russian Academy of Sciences, 10-1 Bol'shaya Gruzinskaya St., Moscow, 123242, Russia

HIGHLIGHTS

- A model explaining distinct mechanisms of the emergence of criticality is developed.
- All the mechanisms indicate spatial synchronization to be crucial for criticality.
- Purely random dynamics is shown to have nothing to do with critical behavior.
- Critical events of any nature are surmised to appear via one of the found mechanisms.

ARTICLE INFO

Article history:
Received 8 August 2018
Received in revised form 7 April 2019
Available online 30 April 2019

Keywords:
Stochastic dynamical systems
Fractal analysis of time series
Coherence analysis
Collective behavior
Critical states
Mechanisms of transition to criticality
Loss of complexity/chaoticity

ABSTRACT

We study diverse mechanisms of the transition of stochastic dynamical systems to critical states. We begin from employing two independent quantitative methods of time series analysis, first-order detrended fluctuation analysis and multivariate canonical coherence analysis, and investigate GPS data of land surface displacements. We find out that there are two different mechanisms of the transition to criticality: the first mechanism is consistent with that observed in some biological dynamical systems and associated with a growth of the energies at low frequencies in the power spectrum, whereas the second mechanism is new and governed by a decay of the energies at high frequencies. Despite this difference, we show that both mechanisms lead to a loss of chaoticity in the system's behavior and result in a more deterministic evolution of the system as a whole. Basing on these findings, we develop a multivariate stochastic model that qualitatively explains both empirically observed mechanisms. The obtained results allow to pose a hypothesis that, in spite of the spread understanding, in stochastic dynamical systems of any nature the transition to a critical state is always realized through a trending nonlinear process that has nothing to do with purely random dynamics.

1. Introduction

Identification of critical states in open stochastic dynamical systems, i.e. precatastrophic states on the eve of abrupt essential changes—catastrophes—in the system's evolution, is a crucial task in many practical applications. Such an identification has to be done at an early stage in order for all possible measures could be taken to minimize, or even avoid, negative consequences of the forthcoming critical event—the catastrophe.

* Corresponding author at: Sceptica Scientific Ltd, Carpenter Court, 1 Maple Road, Bramhall, Stockport, Cheshire SK7 2DH, UK.
E-mail addresses: denis.filatov@sceptica.co.uk (D.M. Filatov), lyubushin@yandex.ru (A.A. Lyubushin).
URLs: https://www.sceptica.co.uk (D.M. Filatov), http://www.alexeylyubushin.narod.ru (A.A. Lyubushin).

https://doi.org/10.1016/j.physa.2019.121309
0378-4371/

After the invention of self-organized criticality (SOC) in 1987 [1,2], critical events in complex stochastic dynamical systems have often become qualitatively likened to sand avalanches occurring over the surface of a sand pile to which one regularly adds grains, one by one, in a random manner. When the number of grains at a given point on the surface exceeds a critical threshold, a sand avalanche—the critical event—of a certain size occurs. In SOC it is stated that since the avalanches appear due to the random external actions, the criticality, as the system's readiness to evince a (pre)catastrophic behavior, is an unpredictably manifesting property of any stochastic system.

We only partly agree with such an understanding of critical phenomena.

Specifically, we admit that there may be reasonable grounds in favor of self-organization in complex systems indeed, in the sense that the system's numerous constituents, being exposed to the influence of random external forcings, can hierarchically demonstrate sophisticated collective behaviors through nonlinear interactions between each other at various spatial scales. In practice this is manifested in various self-similar (power-law-like) dependencies of the observables indicating a persistent or an antipersistent character of the long-term dynamics of the system.

However, we do not share the opinion that the resulting critical events occur randomly and are thus unpredictable. Although for every system there may be numerous random factors that participate in the preparation of a critical event, SOC's schema disregards the fact that during the accumulation of the influence of those factors (the "regular addition of grains to the sand pile") the system may demonstrate certain detectable changes in its evolution until the critical threshold is reached and the critical event occurs. From here it follows that, in our opinion, criticality is not an immanent property inherent to complex stochastic systems. Instead, during the evolution each system transits back and forth between noncritical (quiet, far from catastrophes) and critical (precatastrophic) states.

The point is that for a large number of real stochastic dynamical systems the governing equations of motion are unknown, so that it only remains to statistically analyze historical records of the system's evolution with the purpose to find hidden regularities in the behavior. These regularities can serve as flags of the transition of the dynamical system to a critical mode foregoing a catastrophe. The statistical investigation of the system's historical records leads to time series analysis methods.

For the last 20–25 years fractal analysis of time series has widely been employed in medical and biological applications [3–13]. Intensive research studies in finance based on fractal analysis methods have also been carried out [14–21]. A number of papers on geophysical applications, including those dedicated to the search for precursors of seismic catastrophes, have been published [22–34]. Independently of the specific nature of a dynamical system, it has now become a common point of understanding of critical events that the transition to a precatastrophic state can be realized either via a growth of the energies at low frequencies in the power spectrum, thereby leading to a more deterministic behavior (the 1st mechanism), or via a growth of the energies at high frequencies, resulting in even a more chaotic dynamics (the 2nd mechanism) [4,5,7,9,11]. The reason for such an understanding is a large amount of empirical evidence that when a system is transiting to a critical mode, the statistical characteristic used to quantify its behavior, e.g. a detrended fluctuation analysis (DFA) exponent, either increases—which really corresponds to a more deterministic regime of evolution, or decreases—which is typical for a more chaotic behavior. However, in the recent paper [35], when analyzing a geophysical dynamical system—the Earth's crust, we encountered that it actually exhibits a yet another (the 3rd) mechanism of the appearance of criticality: although the DFA-based exponent decreased, the influence of the energies at high frequencies in the power spectrum also diminished, thereby leading to a more deterministic evolution. To the best of our knowledge, such a mechanism of the transition to a critical state has not been observed in the previous studies.

In [35] the 3rd mechanism was only reported, but no theoretical explanation on its possible origins was given. The aim of this study is to provide more insight on the possible origins of the emergence of the diverse mechanisms of the transition of dynamical systems to critical states.

To this end, we first perform two independent types of stochastic analysis of geophysical time series recorded by GPS stations and show that the new mechanism reported in [35] was not an artifact specific for a particular region (namely, the Japanese islands) but it really takes place in the whole dynamical system—the Earth's crust; besides, we demonstrate that the 1st and the 3rd mechanisms lead to a decrease of the overall complexity of the system's dynamics.

Next, having established the genuine diversity of the mechanisms of the emergence of criticality, we proceed to theoretical analysis and suggest a vector autoregressive stochastic model that is shown to nicely simulate two of the three previously reported mechanisms and yet covers both modes of evolution, critical and noncritical. In doing so, we involve the approach invented by Haken [36] by supplying our model with control parameters responsible for the diversity of modes of the system's behavior. Furthermore, afterward we also pose a hypothesis that the commonly accepted understanding of the transition to criticality via a *growth* of the energies at high frequencies resulting in a more chaotic dynamics before a catastrophe—the 2nd mechanism—may be incorrect. In other words, we suggest that a purely random process quantified by a decay of DFA exponents has nothing to do with critical behavior, and it is exactly a *decay* of the energies at high frequencies, i.e. a more deterministic (or trending) process realized via the 3rd mechanism, that leads systems to precatastrophic states.

The two qualitatively distinct kinds of changes with the energies at high frequencies both leading to a decrease of the DFA exponents immediately raise an important question on the number of crossovers in the power spectrum that, in our opinion, has been overlooked in the previous studies. We show that the decay of high frequencies' energies is accompanied with a greater number of crossovers, and this is exactly the case reported in [35]. We hypothesize that the same, nonlinear, more trending behavior rather than white-noise-like dynamics takes place on the eve of catastrophes in biological dynamical systems as well.

The paper is organized as follows. In Section 2 we first briefly introduce the general idea of fractal analysis of time series and then apply it to quantify the behavior of land surface displacements in California and Japan, using some GPS data from our recent studies. We come to a preliminary conclusion that the overall chaoticity (or complexity) of the dynamical system in a critical state always decreases, which must be reflected in a growth of collective behavior of the system as a whole. In Section 3 we verify that supposition on the same real data using canonical coherence analysis. In Section 4 we develop a stochastic model which explains both previously reported mechanisms by allowing to simulate various types of critical and noncritical dynamics depending on the values of control parameters. In Section 5 we outline a plan for future research. In Section 6 we conclude the paper.

2. Fractal analysis of time series

Let $\{\Delta x_k\}_{k=1}^N$ be a finite sample of a time series of increments of a quantity $x(t)$ defined on the interval $[t_0, t_N]$ with the constant time step $\Delta t = t_k - t_{k-1}$. Depending on the application the quantities $x(t)$ and Δx_k have specific physical meanings, e.g. for GPS time series $x(t_{k-1})$ is the coordinate of a given point of the land surface at the time moment t_{k-1}, while Δx_k is, up to the factor $1/\Delta t$, the velocity of the displacement of that point from $x(t_{k-1})$ to $x(t_k)$ over the corresponding time interval $[t_{k-1}, t_k]$.

Fractal analysis of time series implies introducing the quantity $j \geq 1$ called 'scale' and subsequent partitioning the time interval $[t_0, t_N]$ into several adjacent segments of the size $2j\Delta t$, so that the number of the segments is $n = \frac{N\Delta t}{2j\Delta t}$. Then at each scale j we can define the measure of chaoticity of the system's evolution on the interval $[t_0, t_N]$ as follows

$$D = \frac{\ln \mu(j + \Delta j) - \ln \mu(j)}{\ln(j + \Delta j) - \ln j}. \tag{1}$$

Here the quantity $\mu(j)$ is the data measure at the scale j, while Δj is the scale increment. For the data measure in (1) it holds

$$\mu(j) = \left[\frac{1}{n}\sum_{k=1}^{n}\left(R_k^{(j)}\right)^q\right]^{1/q}, \qquad q \geq 1, \tag{2}$$

where

$$R_k^{(j)} = \left[\frac{1}{N/n}\|\mathbf{r}_k^{(j)}\|_p^p\right]^{1/p}, \qquad p \geq 1. \tag{3}$$

The parameters p and q are considered to be fixed, and they solely define a concrete pair of norms. Usually one takes $p = q = 2$ or $p \to +\infty$, $q = 1$, although other values can also be used. For the components of the vector $\mathbf{r}_k^{(j)} = \left\{r_{k,m}^{(j)}\right\}$ different formulas can be employed. A typical choice is

$$r_{k,m}^{(j)} = \sum_{i=1}^{m}\left(\overline{\Delta x^{(k)}} - \Delta x_i^{(k)}\right), \qquad m = 1, \ldots, \frac{N}{n}, \tag{4}$$

where

$$\overline{\Delta x^{(k)}} = \frac{1}{N/n}\sum_{i=1}^{N/n}\Delta x_i^{(k)} \tag{5}$$

and

$$\Delta x_i^{(k)} = \Delta x_l, \qquad l = (k-1)\frac{N}{n} + i, \tag{6}$$

which yields the conventional first-order detrended fluctuation analysis (DFA) method [37]. For the measure of chaoticity D computed via (4) the notation H_{DFA} is used.

Because the measure of chaoticity is a function of the time series $\{\Delta x_k\}$, depending on the measure's values the entire evolution of a dynamical system can be classified into critical and noncritical states via processing the time series in a moving window of the length N and subsequent analyzing the evolution of the measure of chaoticity.

Remark 1. By calling D the "measure of chaoticity", we follow [38] where the "norm of chaos" was introduced to differentiate between degradation and self-organization processes in open stochastic systems (see also [39]). This parameter should not be considered as a measure of deterministic chaos nor does it have any relation to the Lyapunov exponents that usually appear when studying nonlinear but purely deterministic dynamical systems. We emphasize that the measure of chaoticity D is aimed to quantify persistence/antipersistence in stochastic dynamical systems, that is the systems whose (often unknown) equations of motion contain both a deterministic and a random (stochastic) terms. Therefore, it can also interchangeably be called the "measure of complexity" (see, e.g., [7,9]). ■

Recently the first-order DFA was modified: in [40] it was shown that if instead of (4) one assumes $m = 1, \ldots, \frac{N}{n} + 1$ and takes

$$r_{k,m}^{(j)} = \frac{1}{2}\left(\sum_{i=m+\frac{N}{2}}^{m+\frac{N}{2}+j-1} \Delta x_i^{(k)} - \sum_{i=m+\frac{N}{2}-j}^{m+\frac{N}{2}-1} \Delta x_i^{(k)}\right), \tag{7}$$

then the resulting measure of chaoticity will provide a higher (up to 50%) accuracy of discrimination of critical and noncritical states of a dynamical system. The physical meaning of the difference of the two sums in (7) is the pure acceleration (at the node m within the segment k, at the scale j), while the meaning of the expression (4) is a mixture of velocities and accelerations. Since the modified method is superior over the conventional DFA, in this work we will use the measure of chaoticity computed via (7), and will be denoting it as $\widetilde{H}_{DFA}$. More details on the comparison of the two methods can be found in [40].

We have applied the developed measure of chaoticity $\widetilde{H}_{DFA}$ to the time series of GPS displacements of the land surface in Japan and California, preliminarily filtered from various kinds of non-tectonic perturbations such as orbital errors, atmospheric disturbance, temperature fluctuations etc., and available at the Nevada Geodetic Laboratory [41]. The time series were processed in a moving window of the length $N = 8192$ records (28.4 days) with a time shift 288 records (one day). For the norms in (2)–(3) we had $p \to +\infty$, $q = 1$, while the scales varied exponentially from $j = 1$ to $j = 2048$ as $j = N2^{-(i+1)}$, where $i = 1, \ldots, 12$ was the scale index. Detailed analyses of current seismic hazards with full-color maps of both regions can be found in [35,42]. Here, as a basis for the subsequent topic-independent analysis, we merely provide typical results of the data processing from some GPS stations.

Specifically, the stations J172 and J203 (the Tohoku region, Japan) are located in the areas where earthquakes of the moderate to large magnitudes 6.1 to 6.9 occurred in 2016 [43], while the stations J866 and J105 (northern part of Hokkaido island, Japan) are located in seismically quiet areas [35]. This difference in the seismic activity is clearly seen in Fig. 1: the power spectra of the J172 and J866 northward component time series coincide only at high frequencies, while at low frequencies the spectrum's energies are greater in the critical state; on the other hand, the power spectra of the J203 and J105 upward component time series coincide at low frequencies, whereas at the middle and high ones the energies' influence in the critical state is smaller compared to the noncritical state. These changes of the power spectra taking place in the critical states result in the appearance of crossovers—the critical (or boundary) frequencies ω_B that separate the two parts of the spectra. The fractal measure of chaoticity $\widetilde{H}_{DFA}$ allows to quantify the difference between the critical and noncritical states, as shown in the graphs of the data measure $\mu(j)$ against the scale j: according to (1), the quantity $\widetilde{H}_{DFA}$ is the slope of the straight line in the corresponding log–log plot. Due to a linkage between the spectral and fractal approaches, the critical frequency ω_B in the power spectrum results in the emergence of the critical scale $j_B = \frac{1}{2\omega_B}$, i.e. the border between the two parts of the scale range that separates the major and minor scales, in which the quantity $\widetilde{H}_{DFA}$ has different values [35,42].

Analogous results were obtained for California [42]. In order to visualize the difference between critical and noncritical states in an even more obvious manner, in Fig. 2 we show power spectra for a single GPS station (P305, about 70 km north-west of Fresno) which was experiencing both states during the period from January 2015 to June 2016. As it is seen, in the seismically quiet (noncritical) state the power spectrum demonstrates a rather small change of slope at the critical frequency ω_B; in turn, the measure of chaoticity at the critical scale j_B changes insignificantly, from 0.955 (at the minor scales) to 1.051 (at the major scales) [42]. However, in the seismically active (critical) state the power spectrum's slope changes substantially, following the measure of chaoticity's essential change from 0.976 to 0.356. An evident crossover appears between the low and middle frequencies at $\omega_B \approx 0.01$, thereby making the spectrum flatter in the range $0.01 \ldots 0.04$ when the system is in the critical regime, while in the noncritical mode the crossover is harder to recognize—the spectrum is nearly a straight line close to a power law (see also the spectra in Fig. 1, bottom).

From Fig. 2 an important qualitative observation can be made. In the bottom plot we show the relation between the power spectra in the noncritical and critical modes. Remarkably, despite the decrease of the measure of chaoticity at the major scales in the critical regime from 1.051 to 0.356, the power spectrum at the low frequencies remains unchanged compared to that in the noncritical state—the ratio between the energies is close to 1. Instead, we see that due to the flat part of the spectrum between $\omega \approx 0.01$ and $\omega \approx 0.04$ the influence of the middle and high frequencies in the critical state decreases—the ratio is several times greater than 1. Consequently, when the system transits from the noncritical to the critical regime, the ratio between the energies of the low and high frequencies grows, similarly to how it would do if the measure of chaoticity in a critical regime increased and the influence of low frequencies in the power spectrum grew leaving the energy at high frequencies unchanged, as it normally occurs in some biological dynamical systems (e.g., heart rate dynamics [10,11]) and in horizontal GPS land surface displacements (Fig. 1, top). The same effect takes place for upward GPS data recorded in Japan (Fig. 1, bottom) and other regions of the planet [35]. This observation suggests that the overall chaoticity (or, as it is also referred to, complexity [7,9]) of the system's behavior in a critical mode always decays independently of the specific mechanism of the transition to criticality.

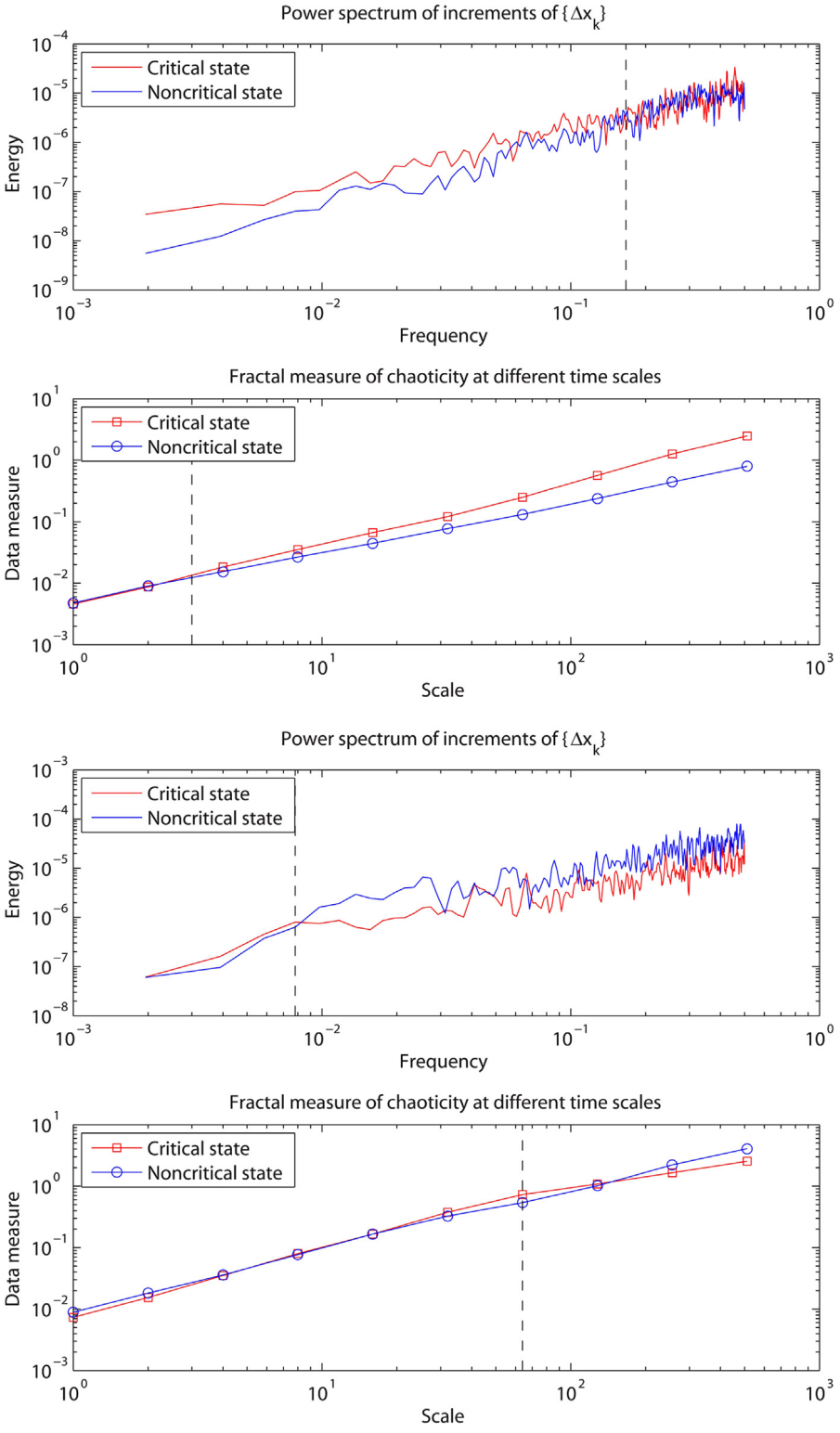

Fig. 1. In the top—power spectra of the northward component of the time series of increments between $\{\Delta x_k\}$ of the Japanese GPS stations J172 (critical state) and J866 (noncritical state) (first plot) and the corresponding dependencies of the data measures $\mu(j)$ on the scale j (second plot); in the bottom—similar outcomes for the upward component of the stations J203 (critical state) and J105 (noncritical state). The vertical dashed lines mark the crossovers—the critical frequencies ω_B and critical scales j_B. Different values for $\widetilde{H}_{DFA}$ at the major and minor scales are due to the different slopes of the straight lines at both sides of j_B.

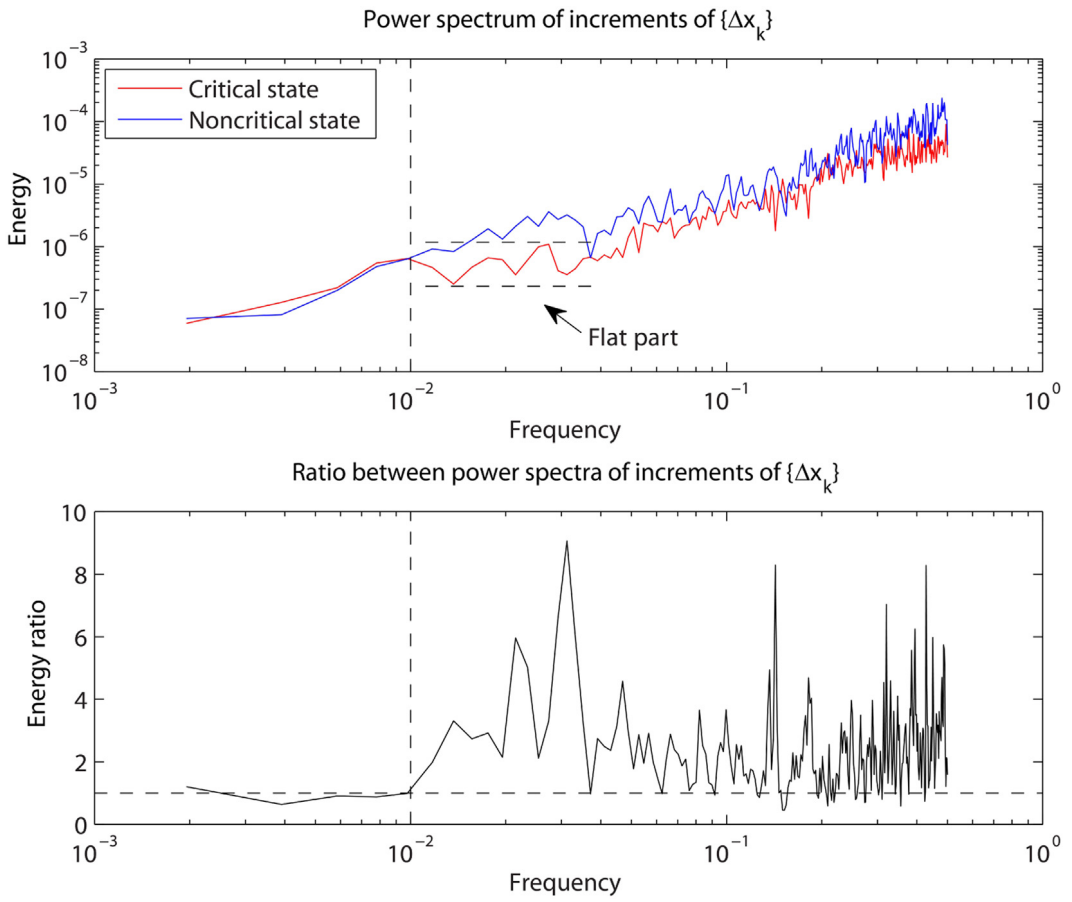

Fig. 2. Power spectra of the upward component of the time series of increments between $\{\Delta x_k\}$ of the U.S. GPS station P305 at two different states of the system's behavior (top) and the ratio between the spectra (bottom) at $N = 2048$. The vertical dashed line marks the critical (or boundary) frequency ω_B.

3. Canonical coherence analysis of time series

Let us note that the decay of chaoticity in a dynamical system is equivalent to the growth of collective behavior between its nearby parts [44]. Hence, the empirically observed loss of complexity should result in a more synchronized evolution of time series recorded at neighboring GPS stations. This consideration suggests that an appropriate method of multivariate analysis would allow to properly distinguish seismically active and quiet areas (or critical and noncritical states) by means of investigation of mutual spectral properties of the time series.

Canonical coherence analysis (CCA) is a suitable tool for this task. It is based on the same idea as canonical correlation analysis [45], except that the coherence coefficient is calculated for the Fourier-transformed data (i.e. in the frequency domain) rather than for the original time series (supplied in the time domain) [46]. In the special case of bivariate time series canonical coherence analysis reduces to the well-known magnitude-squared coherence technique that implies the study of the power cross-spectrum of two scalar (univariate) time series [47]. The coherence coefficient characterizes the presence of harmonics common to all the time series, and it can informally be thought of as the correlation coefficient between the multivariate data at a given frequency.

Let $\{\mathbf{\Delta x}_k\}_{k=1}^N = \{(\Delta x_k^{(1)}, \ldots, \Delta x_k^{(p)})\}_{k=1}^N$ be a finite sample of a p-variate time series. According to the canonical coherence analysis method, the number

$$c_l(\omega) = \frac{\mathbf{S}^*_{\mathbf{\Delta x}\Delta x^{(l)}} \mathbf{S}^{-1}_{\mathbf{\Delta x}\mathbf{\Delta x}} \mathbf{S}_{\mathbf{\Delta x}\Delta x^{(l)}}}{S_{\Delta x^{(l)}\Delta x^{(l)}}} \tag{8}$$

is the partial coherence coefficient between the $(p-1)$-variate time series $\{(\Delta x_k^{(i)})\}$, $i \neq l$, and the univariate time series $\{\Delta x_k^{(l)}\}$ at the frequency ω [25]. In (8) $\mathbf{S}_{\mathbf{\Delta x}\mathbf{\Delta x}}$ is the $(p-1)\times(p-1)$ matrix whose elements $s_{ij}(\omega)$ are the power cross-spectra of the scalar time series $\{\Delta x_k^{(i)}\}$ and $\{\Delta x_k^{(j)}\}$, $\mathbf{S}_{\mathbf{\Delta x}\Delta x^{(l)}}$ is the $(p-1)\times 1$ matrix with the elements power cross-spectra of

the scalar time series $\{\Delta x_k^{(i)}\}$ and $\{\Delta x_k^{(l)}\}$, $\mathbf{S}^*_{\mathbf{\Delta x}\Delta x^{(l)}}$ is its conjugate transpose and $S_{\Delta x^{(l)}\Delta x^{(l)}}$ is the power spectrum of the lth variate at the frequency ω. The superscript '-1' prescribes to take the inverse matrix. Note that an essential requirement of using CCA is stationarity of the time series. In order to satisfy this condition, before using formula (8) we pass from the velocities $\{\mathbf{\Delta x}_k\}$ to the accelerations $\{\mathbf{\Delta}(\mathbf{\Delta x})_k\}$ naturally defined as

$$\Delta(\Delta x)_k^{(i)} = \Delta x_{k+1}^{(i)} - \Delta x_k^{(i)}, \qquad i = 1, \ldots, p, \tag{9}$$

so that the subsequent canonical coherence analysis is performed with respect to the quantities (9). (Observe that DFA-based methods intrinsically incorporate similar procedures, e.g. through (4) or (7), which makes those methods applicable for studying nonstationary time series as well.)

In order to determine the mutual coherence coefficient between all the univariate time series, we apply (8) for computing the partial coherence c_i between every single variate and the remaining $p-1$ time series, and then introduce the quantity

$$C(\omega) = \prod_{i=1}^{p} c_i(\omega). \tag{10}$$

Since all the partial coefficients $c_i \in [0, 1]$, the same holds for (10). Furthermore, due to the multiplication of the partial coefficients, the values of $C(\omega)$ at the frequencies that are not common for all the scalar time series will decay, providing maximum only for the frequencies common for all the p variates [25–27,32].

With the aim to verify the preliminary conclusion made in Section 2 that the overall complexity in a critical state always decreases, we have applied CCA to compute the mutual coherence between several univariate time series produced by five GPS stations closest to a given spatial point. Each of the time series was transformed using (9) and then processed through (8) (for estimating the spectra we employed Welch's method [48]) in a moving window of the same length and time shift as in Section 2. At every time shift we thus calculated a coherence spectrum (10) that quantified the degree of spectral similarity (or synchronization) between the scalar time series at the corresponding time moment. Subsequent averaging of the resulting spectro-temporal field over the whole time period yielded the mean coherence spectrum between the GPS stations' data. The closer the spectrum's value to 1 at a certain frequency, the more coherent the scalar components of the multivariate time series, and hence the more synchronized temporal behavior of the system in the nearby spatial area takes place.

We have analyzed several groups of time series from areas in the Japanese islands and California exhibiting diverse degrees of the seismic hazard. As in the previous section, we used the results of [35,42] and selected GPS data that corresponded to horizontal and vertical motions of the Earth's crust in seismically active and quiet areas. For the former we investigated areas around Los Angeles, the Tohoku region and Shizuoka Prefecture; for the latter we considered areas in the northern part of Hokkaido island and between the cities of Fresno and Bakersfield. The resulting mean coherence spectra are shown in Fig. 3. As it is seen, independently of the region of the planet—and more, regardless of the specific mechanism of transition to criticality,—the critical regimes are accompanied with a growth of the mutual coherence between the univariate time series from the neighboring GPS stations. It is crucial to emphasize that the growth occurs in a wide frequency range, embracing low frequencies (roughly, including $\omega < 0.05$). If this was not so, i.e. if the growth of coherence was observed at high frequencies only, then one could argue that the transition to criticality goes in parallel with an increase of the overall chaoticity of the system. However, it is exactly at the middle and especially at the low frequencies that the mutual coherence in the critical state exceeds that in the noncritical regime. Consequently, not only the increase of collective behavior is caused by the synchronized motions of the closely located parts of the dynamical system, but in both types of critical regimes we are observing a more deterministic, or, equivalently, less chaotic behavior.

4. Multivariate stochastic model for critical and noncritical states

The obtained results impel to design a multivariate evolutionary model that would provide an explanation to the two mechanisms of transition of dynamical systems to critical modes. In other words, we intend to gain insight into how exactly spatial synchronization leads to the appearance of critical phenomena. With this purpose consider a vector autoregression model of order q (VAR(q)-model) of the form

$$\mathbf{z}_k = \sum_{l=1}^{q} \mathbf{A}_l \mathbf{z}_{k-l} + \mathbf{e}_k. \tag{11}$$

Here $\{\mathbf{z}_k\} \equiv \{\mathbf{\Delta}(\mathbf{\Delta x})_k\}$ is the p-variate time series, $\mathbf{A}_l = (a_{ij,l})$ are the regression matrices of the size $p \times p$ that determine the auto- and cross-regressions at the time lags l between the scalar components $\{z_k^{(i)}\}$ and $\{z_k^{(j)}\}$ of the vector time series $\{\mathbf{z}_k\} = \{(z_k^{(1)}, \ldots, z_k^{(p)})\}$, while the vector $\{\mathbf{e}_k\} = \{(e_k^{(1)}, \ldots, e_k^{(p)})\}$'s elements are uncorrelated normally distributed errors [49]. We introduce mutually independent univariate time series $\{\hat{z}_k^{(i)}\}$ with the scaling behavior of the power spectra as a blue noise ($\sim \omega^1$), and define the matrices $\mathbf{A}_l$ via the autocorrelation coefficients

$$r_{ii,l} = \frac{\frac{1}{N}\sum_k \left(\hat{z}_k^{(i)} - \bar{\hat{z}}^{(i)}\right)\left(\hat{z}_{k+l}^{(i)} - \bar{\hat{z}}^{(i)}\right)}{\sqrt{\frac{1}{N^2}\sum_k \left(\hat{z}_k^{(i)} - \bar{\hat{z}}^{(i)}\right)^2 \sum_k \left(\hat{z}_{k+l}^{(i)} - \bar{\hat{z}}^{(i)}\right)^2}},$$

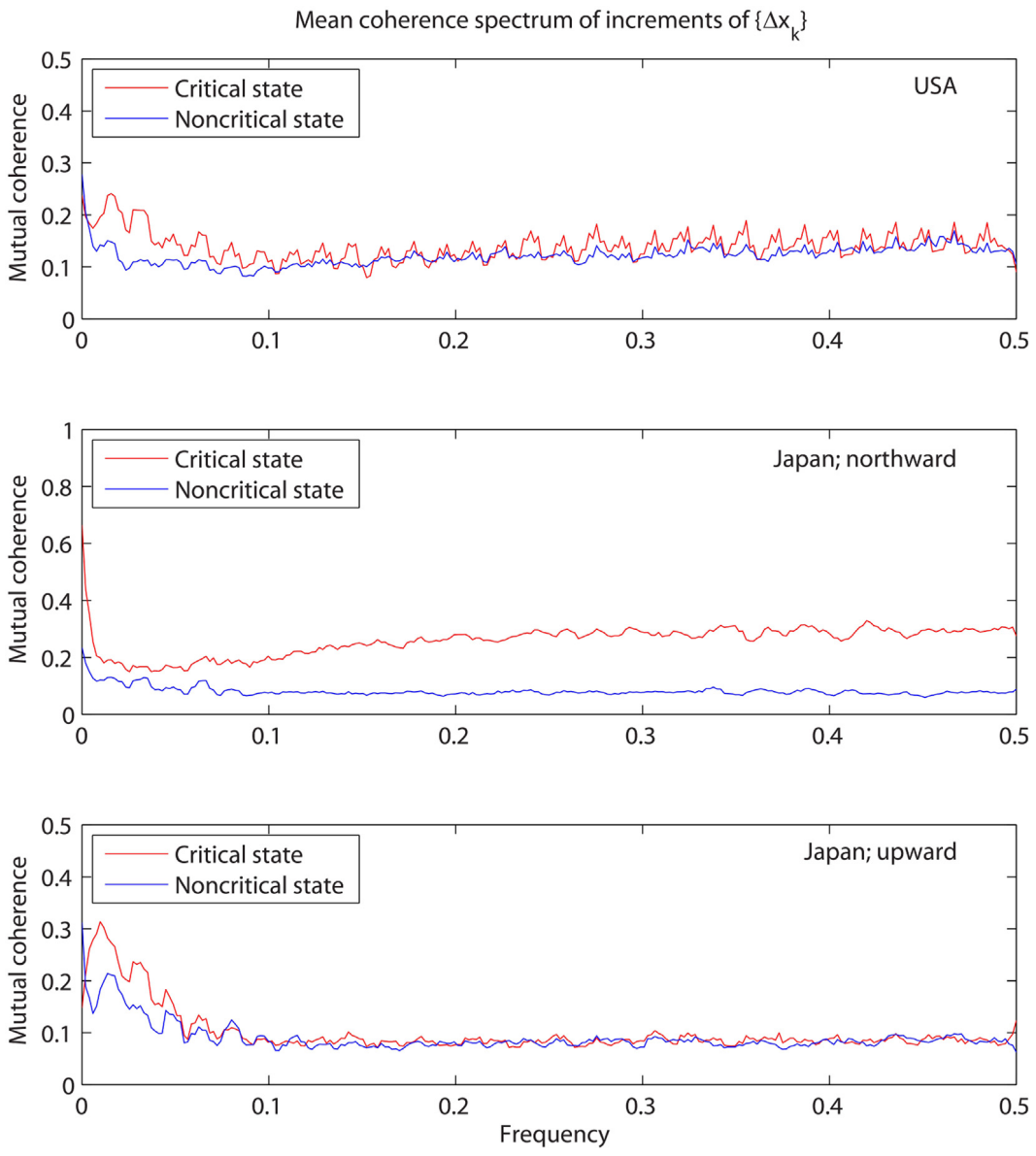

Fig. 3. Mean coherence spectra of five univariate time series of increments between $\{\Delta x_k\}$ from GPS stations in the USA (top) and Japan (middle and bottom) at different system states.

$$i = 1, \ldots, p, \qquad l = 0, \ldots, q, \tag{12}$$

completed with a tuning of the cross-correlations either as

$$r_{ij,l} = r_{ii,l}, \qquad i \neq j, \qquad l = 0, \ldots, q, \tag{13}$$

or as

$$r_{ij,l} = r_{ii,l}\left(1 - \frac{l}{q}\right), \qquad i \neq j, \qquad l = 0, \ldots, q, \tag{14}$$

through the subsequent multivariate Yule–Walker procedure (see, e.g., [48]) additionally supplied with the mutual coherence coefficient $C \in [0, 1]$ as

$$a_{ij,l} = (1 + (C - 1)(1 - \delta_{ij}))a^{\mathrm{YW}}_{ij,l}, \tag{15}$$

where δ_{ij} is the Kronecker delta, $a_{ij,l}^{\mathrm{YW}}$ are the Yule–Walker estimates of the regression coefficients dependent on $r_{ij,l}$. Unlike (10), the quantity C in (15) is simply a number rather than a function of frequency; it is a control parameter (in the sense of [36]) that determines the regime of evolution of the dynamical system. Setting different values for C allows to generate univariate time series $\{z_k^{(i)}\}$ with an arbitrary mutual coherence. Indeed, under $i = j$ it holds $a_{ij,l} = a_{ij,l}^{\mathrm{YW}}$, while under $i \neq j$ we obtain $a_{ij,l} = Ca_{ij,l}^{\mathrm{YW}}$. Consequently, if $C \approx 0$ then $a_{ij,l} \approx 0$, $i \neq j$, and hence the matrices $\mathbf{A}_l$ are close to diagonal, which yields nearly noncoherent univariate time series—the dynamics of each component $\{z_k^{(i)}\}$ is determined mostly by its values at the previous time moments $z_{k-l}^{(i)}$, and hence $\{z_k^{(i)}\}$ are the VAR(q)-versions of the original time series $\{\hat{z}_k^{(i)}\}$ corresponding to a noncritical state of the system; however, if $0 < C \leq 1$ then due to (13)–(14) the cross-regression coefficients $a_{ij,l}$, $i \neq j$, are essentially nonzero, and hence the evolution of every univariate time series $\{z_k^{(i)}\}$ is additionally governed by the other components' values $z_{k-l}^{(j)}$, $i \neq j$, which makes the scalar components $\{z_k^{(i)}\}$ and $\{z_k^{(j)}\}$ mutually coherent, i.e. simulating a critical state.

The core of our model is the tuning of the originally zero cross-correlation coefficients $r_{ij,l}$, $i \neq j$, using (13)–(14) and the subsequent correction of the corresponding cross-regressions $a_{ij,l}$, $i \neq j$, using the control parameter C in (15). These operations are dictated by the earlier observed connection between the loss of chaoticity (which, as we saw in Fig. 3, is accompanied with higher values of the mutual coherence) and the synchronized motions of closely located parts of the dynamical system (which is simulated by the cross-correlations of the univariate time series).

Remark 2. As the control parameter that determines the mutual coherence of the univariate time series, C may, actually, directly affect the cross-correlation coefficients $r_{ij,l}$, $i \neq j$, rather than be applied to the corresponding cross-regressions $a_{ij,l}$, $i \neq j$, after the Yule–Walker procedure as suggested in (15). However, if instead of (13)–(15) we straightforwardly defined $r_{ij,l} = Cr_{ii,l}$ or $r_{ij,l} = Cr_{ii,l}\left(1 - \frac{l}{q}\right)$, $i \neq j$, and afterward computed all $a_{ij,l}$ using the Yule–Walker method, then under $C \approx 0$ the computation of $a_{ij,l}$, $i \neq j$, would generate a numerical exception due to the appearance of singular matrices. Therefore, we take into account the control parameter C *after* the Yule–Walker method via formula (15), which is possible due to a linear dependence between the coefficients $r_{ij,l}$ and $a_{ij,l}$. ■

The physical meaning of formulas (13)–(14) can be understood from the schemas shown in Fig. 4. The modulus of the correlation function shown in blue (left plot, solid curve) corresponds to the noncritical regime of evolution. In this mode the autocorrelation coefficients' absolute values $|r_{ii,l}|$ are large at the small time lags ($l \approx 0$) and properly decay while the time lag is increasing ($l \gg 0$), which results in the power spectrum of the blue noise (right plot, blue solid line $\sim \omega^1$), with smaller energies at low frequencies and larger energies at the high ones. If a critical mode occurs in the way (13)—the cross-correlation function in the absolute value identically coincides with the magnitude of the autocorrelation in the noncritical mode (left plot, Mechanism 1 red solid curve),—then the power spectrum's energies additionally increase compared to the blue noise's spectrum over the whole frequency range (right plot, Mechanism 1 red solid line). In this way Mechanism 1 of the loss of chaoticity (the 1st mechanism from Introduction) is realized (cf. Fig. 1, top), with the single boundary frequency $\omega_B \approx 0.1$. However, if a critical state occurs in the way (14), then the cross-correlation function's magnitude is suppressed at large time lags—under $l \gg 0$ $|r_{ij,l}| \approx 0$, $i \neq j$ (left plot, Mechanism 2 red solid curve),—and therefore, because large l's correspond to low frequencies, the growth of the energies in the power spectrum at low frequencies is not significant compared to the blue noise's spectrum (right plot, Mechanism 2 red solid line). Here a yet another boundary frequency appears, $\omega_B \approx 0.03$. Because for fractal analysis the absolute value of a power spectrum's energy is not important and only its shape counts, we can mentally perform a parallel shift of the resulting power spectrum downward (marked by the dotted arrow on the right plot). As a result, it will match the noncritical's at the low frequencies, but the parts belonging to the middle and high frequencies will get moved below. Consequently, the influence of the middle and high frequencies gets diminished, and in this way Mechanism 2 of the loss of chaoticity (the 3rd mechanism from Introduction) is implemented (cf. Fig. 1, bottom, and Fig. 2, where the more evident boundary frequency is at $\omega_B \approx 0.01$, while the other is at $\omega_B \approx 0.04$ (not marked)). For the sake of giving a reference we also reproduce the case of the white noise $\sim \omega^0$: the autocorrelations coefficients $r_{ii,l}$ are then all zeros except that at $l = 0$ and the resulting power spectrum is of low energy and flat over the entire frequency range (shown by the blue dashed lines in both plots).

In numerical experiments with model (11)–(15) we took $p = 3$, $q = 64$ and first simulated three mutually independent blue noises, $\{\hat{z}_k^{(1)}\}$, $\{\hat{z}_k^{(2)}\}$ and $\{\hat{z}_k^{(3)}\}$, of the length $N = 2048$ records each. After that we calculated their autocorrelation coefficients using (12) and modified the cross-correlations either as (13) (Experiment 1) or as (14) (Experiment 2). Then we applied the multivariate Yule–Walker method to find $a_{ij,l}^{\mathrm{YW}}$, computed $a_{ij,l}$ via (15) with two different values of C, one zero and the other not, and generated $\{\mathbf{z}_k\}$ using (11). Therefore, the resulting VAR(q)-based univariate time series $\{z_k^{(i)}\}$, $i = 1, 2, 3$, were either noncoherent or coherent, depending on the parameter C. In Figs. 5–6 we plot the power spectra of the simulated time series $\{z_k^{(2)}\}$ under $C = 0.5$ (critical mode) and $C = 0$ (noncritical mode). The power spectra of the time series $\{z_k^{(1)}\}$ and $\{z_k^{(3)}\}$ are similar and not shown. We see that formula (13) nicely describes the case of growth of the energies at low frequencies, thus really simulating Mechanism 1 of emergence of a critical state. In its turn, formula (14) provides an outcome analogous to that shown in Fig. 2, that is it corresponds to the case of decay of the energies at high frequencies and therefore explains Mechanism 2 of the loss of complexity reported in Section 2 indeed. In Fig. 7 we also depict the coherence spectra $C(\omega)$ of the simulated time series $\{z_k^{(i)}\}$, $i = 1, 2, 3$, in both regimes. Comparison with

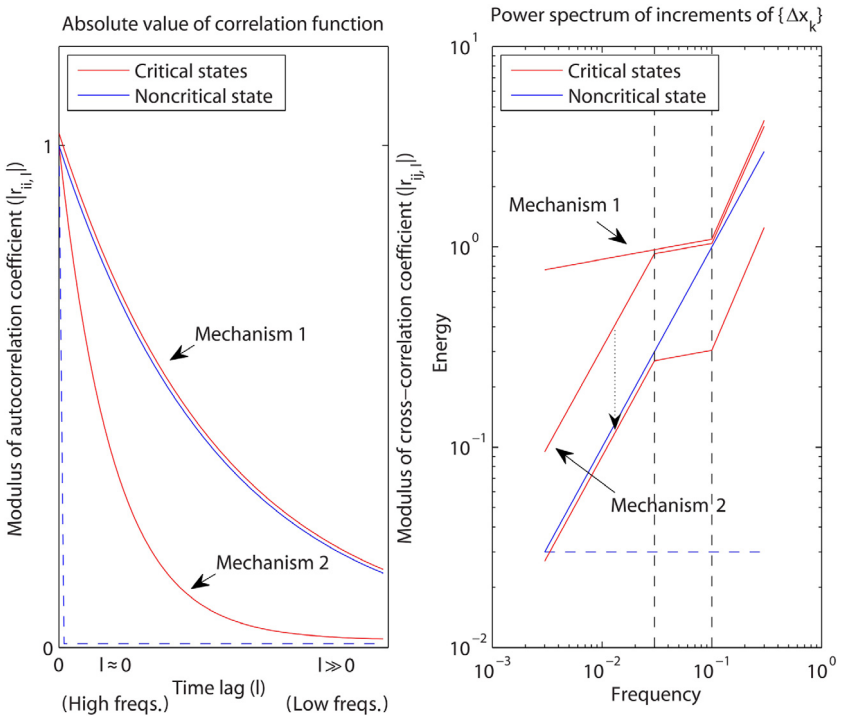

Fig. 4. Qualitative schemas of the absolute values of the correlation functions in diverse modes of the system's behavior (left) and the corresponding power spectra (right) for the autoregression model (11)–(15). In both plots, the colored curves or lines running parallel one to another in fact coincide, but for the sake of clarity they are drawn with tiny gaps. The vertical dashed black lines on the right schema mark the critical frequencies ω_B. See a detailed description in the main text.

Fig. 3 demonstrates that the suggested model reproduces qualitatively the same kind of change of the mutual coherence spectra between the scalar components of the multivariate time series: the transition to a critical state results in a growth of $C(\omega)$ over the frequency range, especially dominant at the frequencies $\omega < 0.1$.

Remark 3. Comparison of Fig. 7 with Fig. 3 also reveals that in reality the noncritical mode of evolution still implies the presence of small nonzero cross-regressions $a_{ij,l}$, $i \neq j$, between the univariate time series $\{z_k^{(i)}\}$ and $\{z_k^{(j)}\}$—otherwise in Fig. 3 we would observe the mutual coherence spectra $C(\omega) \approx 0.1$ over the entire frequency range, including $\omega < 0.1$, as in Fig. 7. This evinces that the scaling behavior of the model power spectra $\sim \omega^1$ over the whole frequency range in a noncritical state is, strictly speaking, an idealization, and a slight deviation from the straight line in the log–log plot, together with a boundary frequency ω_B, should be present. This finding is consistent with the observation made in Section 2 about the values of H_{DFA} in Fig. 2 at the major and minor scales: in the noncritical regime the values on both sides of the boundary scale j_B do differ one from the other (1.051 vs. 0.955), although that difference is not as big as in the critical mode (0.356 vs. 0.976). ■

Figs. 5–7 are an evident proof of the importance of spatial synchronization as a driving force of the loss of chaoticity and emergence of critical states followed by catastrophes in dynamical systems. Hence, the mutual coherence, as a measure of the spatial synchronization, can be considered as a quantitative flag of a forthcoming catastrophe.

5. Remarks for future research

The VAR(q)-model (11)–(15) qualitatively explains both mechanisms of the transition to critical states that we observed when processing the real time series, as well as accounts for both regimes of evolution, critical and noncritical. Nevertheless, it is merely an intermediate solution between what statistical physicists nowadays mainly have—purely quantitative stochastic methods, such as the (uni- or multifractal) DFA techniques, that do distinguish critical and noncritical states of dynamical systems but provide no explanation on the possible origins of that difference—and what they eventually desire to have—the adequate equations of motion which would fully describe the systems' behavior in all possible aspects. The reason why we decided to employ linear vector autoregression is that it is an apt tool for studying the influence of spatial synchronization on the appearance of critical phenomena via cross-correlation coefficients of the univariate time series. Most likely, in reality a more complicated mechanism of the loss of chaoticity compared to (13)–(14) takes place.

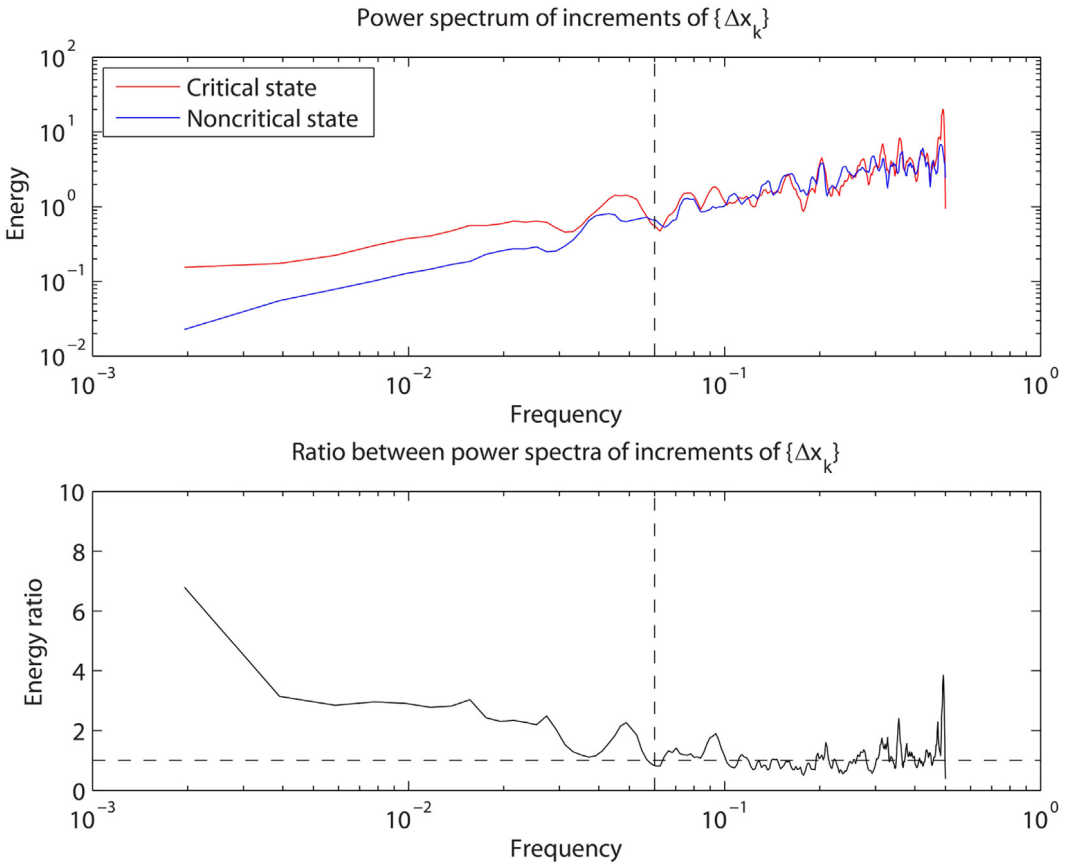

Fig. 5. Power spectra of the univariate time series $\{z_k^{(2)}\}$ simulated by the VAR(q)-model in Experiment 1 (formula (13)) at two different states of the system's behavior (top) and the ratio between the spectra (bottom). Cf. Fig. 1, top.

In this connection, the growth of the number of crossovers in the power spectrum under Mechanism 2 indicates there are more complex interactions between the system's constituents than under Mechanism 1. This suggests that higher-order detrended fluctuation analysis methods could be useful for further investigating the role of spatial synchronization in stochastic dynamical systems [37,50]. In particular, currently we are investigating geophysical time series produced by seismometers with the sample rate 1 Hz. We have found out that at the very small time scales (approx. less than five minutes) the dynamics of the Earth's crust evinces a much more nonlinear behavior before critical events, with multiple crossovers, so that higher-order DFAs are the tools that may help properly quantify it.

Having said all that, as a concluding important remark we would also like to pose a hypothesis aimed to stimulate further studies in the field of stochastic dynamics and critical states of complex systems.

As it is known, in a number of applications (e.g., heart rate dynamics of people with atrial fibrillation, gait dynamics of people with Huntington's disease, among others) DFA-based measures of chaoticity at major scales, similarly to what we reported above for upward GPS displacements, are observed to decrease to ≈ 0.5, which is nowadays commonly interpreted as the transition to criticality via a nearly random process, i.e. through a more chaotic behavior (the 2nd mechanism from Introduction)—see, e.g., [5,7,9]. However, as far as we know, for those applications the question of the structure of the power spectra of the original (not randomly shuffled) time series was not directly investigated. We think, a special research on this issue would clarify the situation, but until then the general observations on the mathematical similarity of the mechanisms of evolution of various stochastic dynamical systems permit us to speculate that the mechanism of the transition to critical states in those applications may be the same as that described above for the vertical GPS displacements, i.e. the 3rd mechanism from Introduction, or Mechanism 2 from Section 4. Besides, one must not fail to bear in mind that although for a truly random process DFA-based methods are known to produce the chaoticity's estimates close to 0.5, the converse must not necessarily hold, and due to the multiple crossovers it does not indeed, as we showed in the previous sections. These observations allow to make a preliminary conclusion that *independently of the nature of a dynamical system the transition to criticality always results in a more deterministic (trending) behavior* because the ratio between the energies at low and high frequencies grows anyway, solely one or another mechanism of transition is

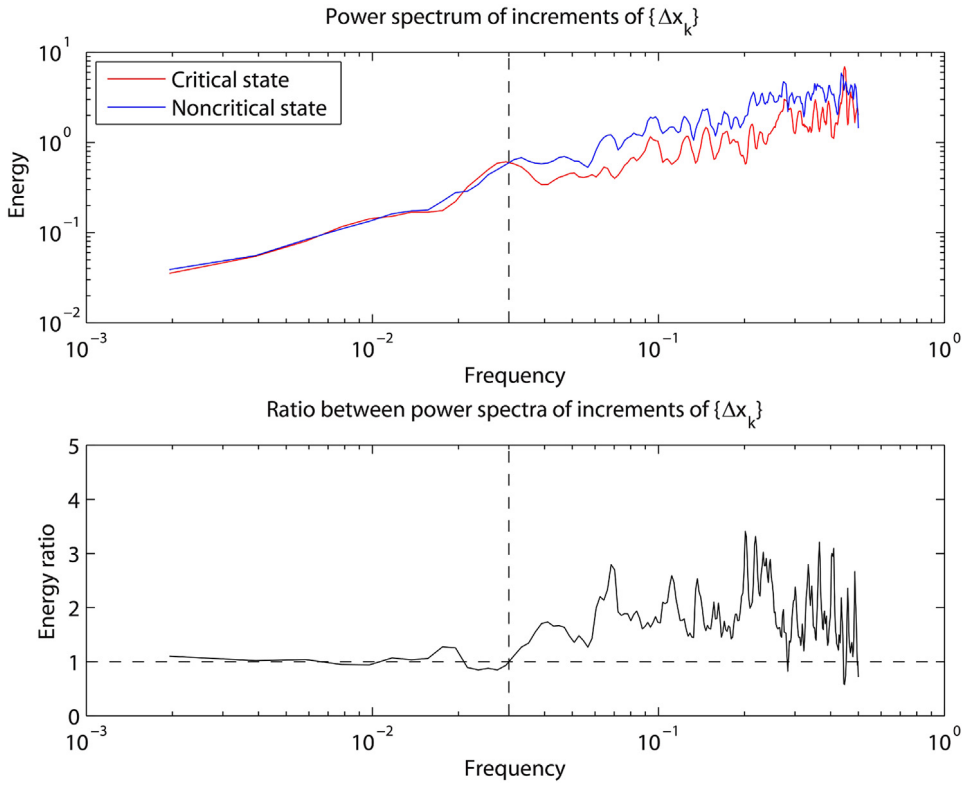

Fig. 6. Power spectra of the univariate time series $\{z_k^{(2)}\}$ simulated by the VAR(q)-model in Experiment 2 (formula (14)) at two different states of the system's behavior (top) and the ratio between the spectra (bottom). Cf. Fig. 1, bottom, and Fig. 2.

realized yielding either an increase or a decrease of the measure of chaoticity. In other words, no evolution toward simple randomness takes place even if the measure of chaoticity decays, and a sophisticated mechanism of nonlinear interactions between the harmonics of different wavelengths likely governs the critical phenomenon. Perhaps, such a mechanism may be related to the nonlinear energy cascades observable in the power spectra of the quantities describing turbulent fluid flows [51]. Anyway, if a future research reveals the same transformation of the structure of the power spectrum for the previously studied biological dynamical systems, that will not affect those studies' practical outcomes but confirm our hypothesis and assist better understanding of the emergence of critical phenomena; otherwise, that will disprove our supposition but simultaneously stress that vertical movements of blocks of the Earth's crust exhibit a new mechanism of transition to critical states that has not been previously reported.

6. Conclusion

We have investigated diverse mechanisms of the transition of stochastic dynamical systems to critical states that had been reported in previous studies. With this aim we employed two independent quantitative methods of time series analysis, first-order detrended fluctuation analysis and canonical coherence analysis, and analyzed GPS data of land surface displacements. We found out that there are two different mechanisms of the transition to criticality: the first mechanism is the same that the one observed in some biological dynamical systems and associated with a growth of the power spectrum energies at low frequencies, whereas the second mechanism is new and governed by a decay of the energies at high frequencies. We showed that both mechanisms lead to a loss of chaoticity in the system's behavior and result in a more deterministic evolution of its neighboring parts. Afterward we developed a vector autoregression stochastic model that qualitatively explains both empirically observed mechanisms, and, given the idea of mathematical similarity of the evolutionary mechanisms in dynamical systems of diverse nature, posed a hypothesis that in any system the transition to a critical state is always a trending nonlinear process having nothing to do with purely random dynamics. Further research efforts are needed to either confirm or disprove the hypothesis posed.

CRediT authorship contribution statement

Denis M. Filatov: Conceptualization, Methodology, Software, Validation, Formal analysis, Investigation, Writing – original draft. **Alexey A. Lyubushin:** Methodology, Data curation, Writing – original draft, Funding acquisition.

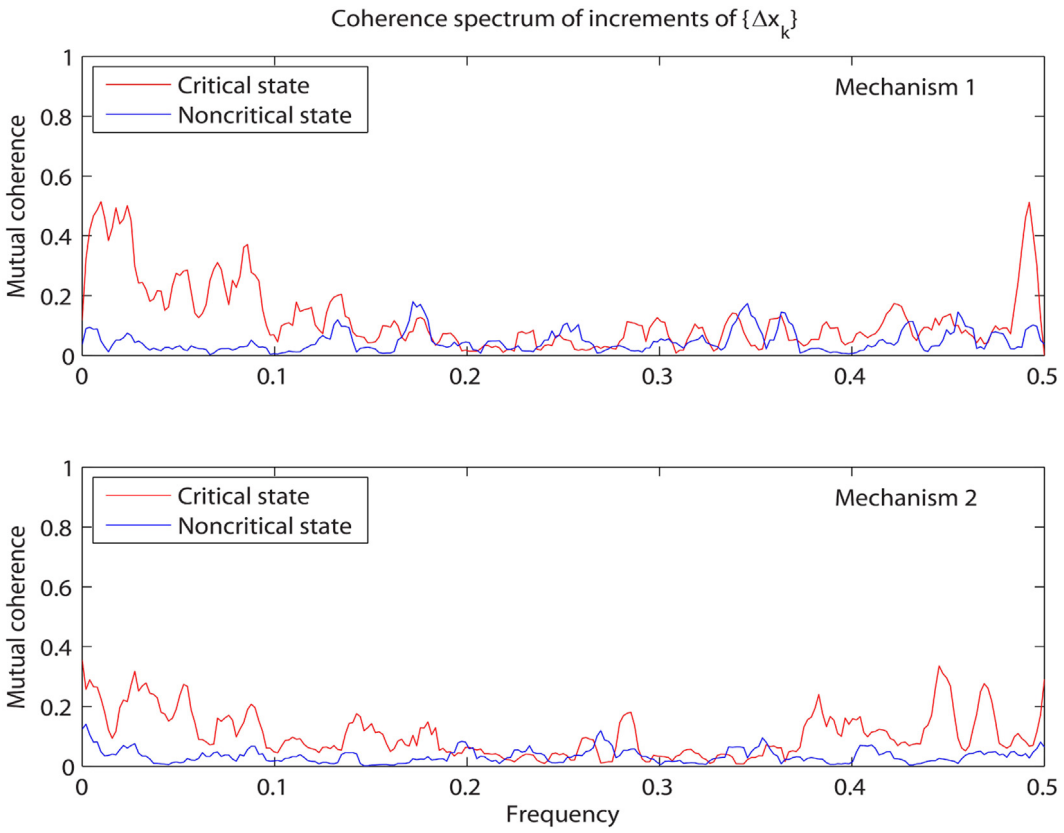

Fig. 7. Coherence spectra of the three univariate time series, $\{z_k^{(1)}\}$ to $\{z_k^{(3)}\}$, simulated by the VAR(q)-model under the mechanisms (13) (top) and (14) (bottom) at different system states.

Acknowledgments

We are grateful to the anonymous reviewers whose comments have contributed to the improvement of the final version of the paper. This research was partially supported by the grant No. 18-05-00133 of the Russian Foundation for Basic Research (RFFI).

References

[1] P. Bak, C. Tang, K. Wiesenfeld, Self-organized criticality: An explanation of the 1/f noise, Phys. Rev. Lett. 59 (1987) 381–384.
[2] P. Bak, How Nature Works: The Science of Self-Organized Criticality, Copernicus (Springer), USA, 1996.
[3] Y. Ashkenazy, P.C. Ivanov, S. Havlin, C.-K. Peng, A.L. Goldberger, H.E. Stanley, Magnitude and sign correlations in heartbeat fluctuations, Phys. Rev. Lett. 86 (2001) 1900–1903.
[4] A. Bunde, S. Havlin, J.W. Kantelhardt, T. Penzel, J.-H. Peter, K. Voigt, Correlated and uncorrelated regions in heart-rate fluctuations during sleep, Phys. Rev. Lett. 85 (2000) 3736–3739.
[5] A.L. Goldberger, L.A.N. Amaral, J.M. Hausdorff, P.C. Ivanov, C.-K. Peng, H.E. Stanley, Fractal dynamics in physiology: Alterations with disease and aging, Proc. Natl. Acad. Sci. USA 99 (2002) 2466–2472.
[6] P.C. Ivanov, L.A.N. Amaral, A.L. Goldberger, S. Havlin, M.G. Rosenblum, H.E. Stanley, Z.R. Struzik, From 1/f noise to multifractal cascades in heartbeat dynamics, Chaos 11 (2001) 641–652.
[7] L.A. Lipsitz, A.L. Goldberger, Loss of 'complexity' and aging: Potential applications of fractals and chaos theory to senescence, J. Am. Med. Assoc. 287 (1992) 1806–1809.
[8] I. Osorio, A.A. Lyubushin, D. Sornette, Automated seizure detection: Unrecognized challenges, unexpected insights, Epilepsy Behav. 22 (2011) S7–S17.
[9] C.-K. Peng, J.M. Hausdorff, A.L. Goldberger, Fractal mechanisms in neuronal control: Human heartbeat and gait dynamics in health and disease, in: J. Walleczek (Ed.), Self-Organized Biological Dynamics and Nonlinear Control: Toward Understanding Complexity, Chaos and Emergent Function in Living Systems, Cambridge University Press, Cambridge, 2000, pp. 66–96.
[10] C.-K. Peng, J.M. Hausdorff, J.E. Mietus, S. Havlin, H.E. Stanley, A.L. Goldberger, Fractals in physiological control: from heart beat to gait, in: M. Shlesinger, G. Zaslavsky, U. Frisch (Eds.), Procs. of the Int. Workshop Held at Nice, France, 27–30 June 1994, in: Lecture Notes in Physics: Lévy Flights and Related Topics in Physics, Springer, Berlin, Heidelberg, 1995, pp. 313–330.
[11] C.-K. Peng, S. Havlin, H.E. Stanley, A.L. Goldberger, Quantification of scaling exponents and crossover phenomena in nonstationary heartbeat time series, Chaos 5 (1995) 82–87.
[12] H. Saghir, T. Chau, A. Kushki, Clustering of time-evolving scaling dynamics in a complex signal, Phys. Rev. E 94 (2016) 012220.

[13] S. Sunderam, S.S. Talathi, A.A. Lyubushin, D. Sornette, I. Osorio, Challenges for emerging neurostimulation-based therapies for real-time seizure control, Epilepsy Behav. 22 (2011) 118–125.
[14] S. Bianchi, A. Pianese, Modelling stock price movements: Multifractality or multifractionality? Quant. Finance 7 (2007) 301–319.
[15] A. Carbone, G. Castelli, H.E. Stanley, Time-dependent Hurst exponent in financial time series, Physica A 344 (2004) 267–271.
[16] T. Di Matteo, Multi-scaling in finance, Quant. Finance 7 (2007) 21–36.
[17] J. Kwapień, P. Oświęcimka, S. Drożdż, Detrended fluctuation analysis made flexible to detect range of cross-correlated fluctuations, Phys. Rev. E 92 (2015) 052815.
[18] K. Kim, S.-M. Yoon, Multifractal features of financial markets, Physica A 344 (2004) 272–278.
[19] J.L. López, J.G. Contreras, Performance of multifractal detrended fluctuation analysis on short time series, Phys. Rev. E 87 (2013) 022918.
[20] R.F. Mulligan, Fractal analysis of highly volatile markets: An application to technology equities, Q. Rev. Econ. Finance 44 (2004) 155–179.
[21] Y. Wang, Y. Wei, C. Wu, Detrended fluctuation analysis on spot and futures markets of West Texas intermediate crude oil, Physica A 390 (2011) 864–875.
[22] R.G. Kavasseri, R. Nagarajan, A multifractal description of wind speed records, Chaos Solitons Fractals 24 (2005) 165–173.
[23] E. Koscielny-Bunde, J.W. Kantelhardt, P. Braun, A. Bunde, S. Havlin, Long-term persistence and multifractality of river runoff records: Detrended fluctuation studies, J. Hydrol. 322 (2006) 120–137.
[24] Q. Li, Z. Fu, N. Yuan, F. Xie, Effects of non-stationarity on the magnitude and sign scaling in the multi-scale vertical velocity increment, Physica A 410 (2014) 9–16.
[25] A.A. Lyubushin, Analysis of canonical coherences in the problems of geophysical monitoring, Izv. Phys. Solid Earth 34 (1998) 52–58.
[26] A.A. Lyubushin, Analysis of multidimensional geophysical monitoring time series for earthquake prediction, Ann. Geophys. 42 (1999) 927–937.
[27] A.A. Lyubushin, G.A. Sobolev, Multifractal measures of synchronization of microseismic oscillations in a minute range of periods, Izv. Phys. Solid Earth 42 (2006) 734–744.
[28] A.A. Lyubushin, Multifractal parameters of low-frequency microseisms, in: V. de Rubeis, Z. Czechowski, R. Teisseyre (Eds.), Synchronization and Triggering: from Fracture to Earthquake Processes, in: Geoplanet: Earth and Planetary Sciences, Springer, Berlin, Heidelberg, 2010, pp. 253–272.
[29] A.A. Lyubushin, Seismic catastrophe in Japan on March 11, 2011: Long-term prediction on the basis of low-frequency microseisms, Izv. Atmos. Ocean. Phys. 46 (2011) 904–921.
[30] A.A. Lyubushin, Prognostic properties of low-frequency seismic noise, Nat. Sci. 4 (2012) 659–666.
[31] A.A. Lyubushin, Dynamic estimate of seismic danger based on multifractal properties of low-frequency seismic noise, Nat. Hazards 70 (2014) 471–483.
[32] A.A. Lyubushin, Analysis of coherence in global seismic noise for 1997–2012, Izv. Phys. Solid Earth 50 (2014) 325–333.
[33] S.M. Potirakis, M. Hayakawa, A. Schekotov, Fractal analysis of the ground-recorded ULF magnetic fields prior to the 11 March 2011 Tohoku earthquake (Mw = 9): Discriminating possible earthquake precursors from space-sourced disturbances, Nat. Hazards 85 (2017) 59–86.
[34] P.A. Varotsos, N.V. Sarlis, E.S. Skordas, Natural Time Analysis: The New View of Time, in: Precursory Seismic Electric Signals, Earthquakes and Other Complex Time Series, Springer, Berlin, Heidelberg, 2011.
[35] D.M. Filatov, A.A. Lyubushin, Fractal analysis of GPS time series for early detection of disastrous seismic events, Physica A 469 (2017) 718–730.
[36] H. Haken, Information and Self-Organization: A Macroscopic Approach to Complex Systems, Springer, Berlin, Heidelberg, 2006.
[37] J.W. Kantelhardt, Fractal and multifractal time series, 2008, http://arxiv.org/abs/0804.0747.
[38] Y.L. Klimontovich, Relative ordering criteria in open systems, Uspekhi Phys. Nauk 39 (1996) 1169–1179.
[39] Y.L. Klimontovich, Statistical Theory of Open Systems: A Unified Approach to Kinetic Description of Processes in Active Systems, Springer, The Netherlands, 1995.
[40] D.M. Filatov, A method for identification of critical states of open stochastic dynamical systems based on the analysis of acceleration, J. Stat. Phys. 165 (2016) 681–692.
[41] Nevada Geodetic Laboratory, University of Nevada, USA 2015, http://geodesy.unr.edu/index.php.
[42] D.M. Filatov, A.A. Lyubushin, Precursory analysis of GPS time series for seismic hazard assessment, Pure Appl. Geophys. (2019) http://dx.doi.org/10.1007/s00024-018-2079-3, in press.
[43] U.S. Geological Survey, Report on the M6.9 Namie, Japan, earthquake of 21 November 2016, 2016, http://earthquake.usgs.gov/earthquakes/eventpage/us10007b88.
[44] D. Sornette, Critical Phenomena in Natural Sciences. Chaos, Fractals, Selforganization and Disorder: Concepts and Tools, Springer, Berlin, Heidelberg, 2006.
[45] H. Hotelling, Relations between two sets of variants, Biometrika 28 (1936) 321–377.
[46] D.R. Brillinger, Time Series: Data Analysis and Theory, Holt, Rinehart and Winston Inc., USA, 1975.
[47] S.M. Kay, Modern Spectral Estimation: Theory and Application, Prentice-Hall Inc., USA, 1988.
[48] S.L. Marple Jr., Digital Spectral Analysis with Applications, Prentice-Hall Inc., USA, 1987.
[49] G.E.P. Box, G.M. Jenkins, G.C. Reinsel, Time Series Analysis: Forecasting and Control, Prentice-Hall Inc., USA, 1994.
[50] P. Oświęcimka, S. Drożdż, J. Kwapień, A.Z. Górski, Effect of detrending on multifractal characteristics, Acta Phys. Polon. A 123 (2013) 597–603.
[51] U. Frisch, Turbulence: The Legacy of A.N. Kolmogorov, Cambridge University Press, Cambridge, 1995.